Synthesis of oriented arrays of TiO_2 nanorods *via* a high temperature conversion of carbon nanotubes†

Ben F. Cottam and Milo S. P. Shaffer*

Received (in Cambridge, UK) 20th June 2007, Accepted 20th July 2007
First published as an Advance Article on the web 15th August 2007
DOI: 10.1039/b709353e

Oriented arrays of both rutile and anatase nanorods have been synthesised in a two-stage process, employing multi-walled carbon nanotubes as the initial structural template.

Carbon nanotubes (CNTs) had been observed on several occasions[1a,b] before their relationship to fullerenes was recognised.[2] However, following Iijima's 1991 paper, the potential to use these hollow, high aspect ratio, structures as templates for fabricating well-defined nanorods (or nanowires) was swiftly realised by a number of groups, who filled the tubes with metals, oxides, and other salts.[3a–d] Lieber and co-workers took an alternative approach; rather than using the carbon as an inert scaffold, they performed reactions to convert multi-walled CNTs (MWCNTs) into silicon and other carbide nanowires, using volatile metal–iodide complexes.[4a,b] Although the reaction involves a volume change, the dimensions of the carbide structures are directly related to the original CNTs. These initial experiments were based on nanotubes grown *via* chemical vapour deposition (CVD),[5] selected for their relative purity despite their imperfect, curly structure and random arrangement. Since then, CVD has been developed to grow highly pure, aligned arrays of relatively straight nanotubes[6a–f] that, in this study, allow templating of structured layers of carbide nanorods; subsequent conversion to titanium dioxide provides material of much greater technological significance.

Titanium oxide nanostructures have also been extensively researched and several synthetic methods for the growth of aligned arrays of TiO_2 nanowires and nanotubes have been established. Synthetic strategies include the use of porous alumina[7a–c] or CNTs[8a–c] as templates for electro-[7a] or sol–gel[7b,8a–c] deposition, seeded growth with either TiO_2 nanoparticles[9] or $TiCl_4$ embedded in mesoporous silica,[10] anodization of titanium film,[11a–d] and metalorganic CVD (MOCVD).[12a,b] These methods all result in polycrystalline materials, often with low aspect ratio, that are not necessarily ideal for applications, which include photovoltaics,[13a,b] photocatalysis,[14] and gas sensors.[15] This communication demonstrates a new strategy for the synthesis of high quality, aligned titania nanorods.

There are three distinct steps in the experimental strategy. Initially, aligned arrays of carbon nanotubes were grown *via* injection CVD.[6e] In brief, a 3 wt% ferrocene–xylene solution was injected at 5 mL h^{-1} into a furnace containing quartz slides at 760 °C, using argon as the carrier gas. After 2 h, the xylene flow was terminated, the furnace cooled, and quartz substrates loaded with oriented CNTs collected.

In the second stage of the synthesis, performed at 800 °C and at a vacuum of $\sim 1 \times 10^{-2}$ mbar, the CNTs were placed in a furnace tube next to an alumina boat containing finely-ground titanium metal (Sigma-Aldrich, 100 mesh, 99.7%). A boat containing iodine (Fisher Scientific, reagent grade) was placed in the furnace tube but outside the main heating zone, allowing a gradual supply of iodine throughout the reaction. In a typical experiment, the mass ratios of the CNTs, iodine and titanium were 1 : 3 : 10, using ~25 mg of CNTs. Although stoichiometrically more iodine is needed, the solid titanium reacts relatively slowly, so is provided in excess. The reactions were performed for up to 10 h although some iodine and titanium still remained. The conversion to carbide proceeds by the reaction with titanium iodide, formed *in situ*:

$$TiI_4(g) + C(s) \rightarrow TiC(s) + 2I_2(g)$$

This reaction is more favourable for the iodide than the corresponding bromide or chloride, and is encouraged by high temperatures. At atmospheric pressure, and 800 °C, the calculated free energies for the conversion are 462, 311, and 105 kJ mol^{-1}, for X = Cl, Br, and I, respectively. The reaction thus requires a reduced pressure in order to proceed.

The final stage of the process is a simple conversion of the carbide to the oxide by heat treatment in air. The oxidations were performed at 525 °C (12 h) and 800 °C (30 min) in an attempt to produce, respectively, anatase and rutile TiO_2. Each stage of the process was characterised by high-resolution transmission electron microscopy (HRTEM, JEOL JEM 2010, operating at 200 kV), scanning electron microscopy (SEM, LEO Gemini FEGSEM, 20 kV), X-ray diffraction (XRD, Philips X'Pert diffractometer with Cu Kα radiation) and Raman spectroscopy (Horiba Infinity, 628 nm laser).

The EM analysis of the as-grown MWCNTs (Fig. 1) shows that the nanotubes are wavy in nature but oriented along their length; they have the usual well-graphitised layered structure with a hollow core. The crystallinity is confirmed by the presence in the selected area electron diffraction (SAED) pattern of the spots derived from the (002) planes of graphitic carbon.

Following conversion of the CNTs, the TiC nanostructures retain the overall shape and alignment of the original template (Fig. 2(a)). Grains of TiC, roughly 10 nm in diameter, are observed, while the graphitic core of the original CNT is still in evidence (Fig. 2(b)). The partial conversion is confirmed by the associated SAED pattern (Fig. 2(c)) in which both graphitic (002)

Department of Chemistry, Imperial College London, South Kensington, London, United Kingdom SW7 2AZ. E-mail: m.shaffer@imperial.ac.uk; Fax: +44 0207 5945801; Tel: +44 0207 5945825

† Electronic supplementary information (ESI) available: Raman spectra and high resolution TEM images of the rutile and anatase products. TEM images of additional conversion reactions performed. See DOI: 10.1039/b709353e

 This journal is © The Royal Society of Chemistry 2007

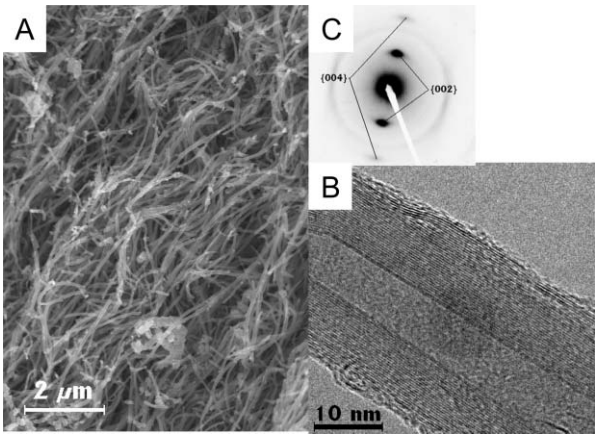

Fig. 1 (a) SEM image of CVD grown MWCNTs, revealing their wavy but oriented nature; (b) TEM image of a single MWCNT; (c) the corresponding SAED pattern.

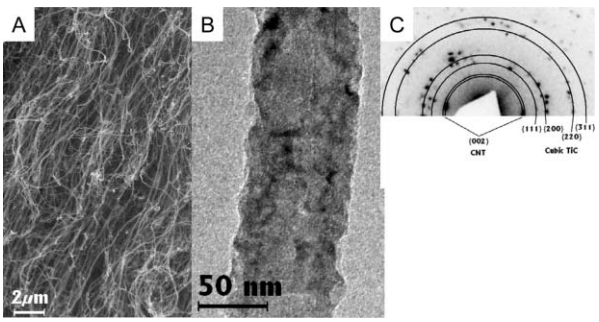

Fig. 2 (a) SEM image of the nanostructures after a partial conversion to TiC; (b) TEM image of a single TiC/CNT nanostructure; (c) the SAED.

and numerous diffraction spots from polycrystalline, cubic TiC can be seen.

After the carbide conversion, the sample remains black, but after the final oxidation steps, the products become white, indicating a change from TiC to TiO_2. SEM and TEM analysis of the final products from oxidations at 800 and 525 °C are shown in Fig. 3. After oxidation, the overall alignment of the structures is again preserved and the individual nanorods have a 'beaded-necklace' appearance. Both products are polycrystalline, with the low and high temperature oxidation generating ~20 nm and ~70 nm grains, respectively. The corresponding SAED patterns confirm the appearance of rutile at 800 °C (Fig. 3(c)) and anatase at 525 °C (Fig. 3(e)). High resolution TEM images of both the rutile and anatase products are provided in the electronic supporting information, ESI,† and confirm the changes in crystallography of the products.

Powder X-ray diffraction of the three stages of the reaction (Fig. 4) supports the TEM results. The initial MWCNTs (Fig. 4(a)) diffract predominantly from the (002) planes at $2\theta = 26°$, as expected. In the intermediate carbide compound (Fig. 4(b)) strong TiC peaks ($2\theta = 36°$, 42°, 61° and 73°) are observed; however, some graphite is retained, due to incomplete conversion, along with some rutile, presumably due to imperfect exclusion of oxygen. The conversion performed at 800 °C results in pure rutile (Fig. 4(d), $2\theta = 27°$, 36°, 39°, 41°, 45°, 54°, 57°, 63°, 65°, 69°, 70°), whereas the conversion at 525 °C results in predominantly anatase (Fig. 4(c),

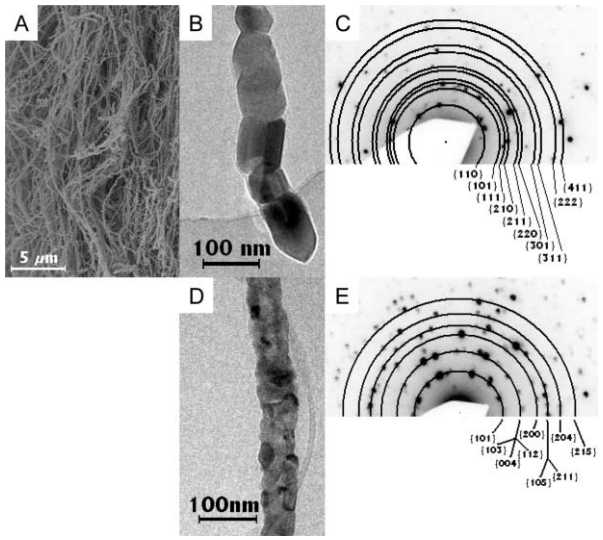

Fig. 3 (a) SEM image of (rutile) TiO_2 nanostructures. TEM images of single (b) rutile and (d) anatase nanorods; (c) + (e) corresponding SAED.

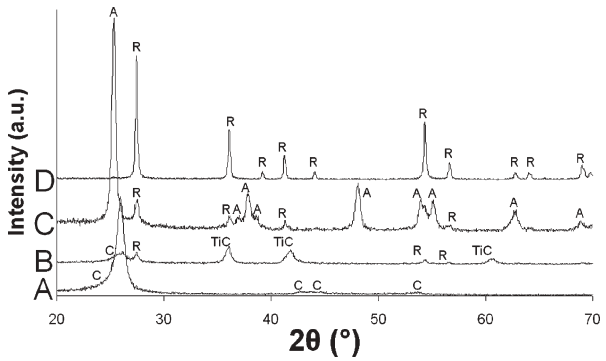

Fig. 4 X-Ray diffraction patterns showing the composition of the nanostructures at each stage: (a) MWCNTs; (b) the carbide product; (c) the oxidation product at 525 °C; and (d) the oxidation product at 800 °C (C, TiC, R and A indicate graphite, TiC, rutile and anatase peaks, respectively).

2θ = 25°, 37°, 38°, 39°, 48°, 54°, 55°, 63°, 69°). The small rutile peaks observed are probably due to retention of the rutile component in the original TiC (estimated to be approximately ~6% from the relative areas under the 25° and the 27° peaks in Fig. 4(c)).

Raman analysis was also performed after each of the three stages (ESI).† The spectrum obtained after stage one exhibits clear graphitic and associated defect peaks at around 1580 and 1300 cm^{-1}, respectively. In the spectrum of the intermediate sample, TiC peaks are observed at 260, 420 and 605 cm^{-1}; however, the graphitic and defect peaks from the remaining CNT material are also still evident, along with a possible overlapping contribution from the small rutile fraction. The titania signals in the final products can be assigned to the standard spectra for anatase and rutile for the low and high temperature oxidation reactions, respectively.

Thermogravimetric analyses (Perkin Elmer Pyris 1) of the carbide product in air, with maximum temperatures of 525 and 800 °C, provide further information about the final conversion

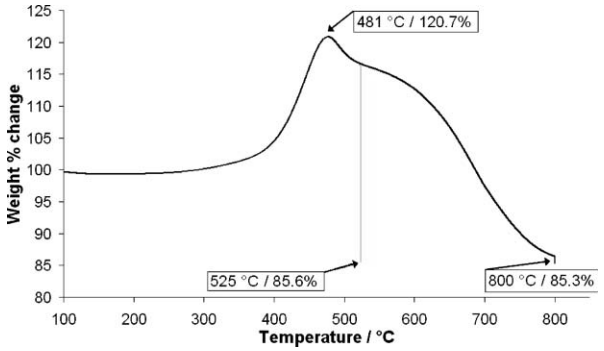

Fig. 5 TGA plot of the conversion of stage two nanostructures (predominantly TiC nanorods) to anatase nanorods at 525 °C (grey plot) and rutile nanorods at 800 °C (black line).

step. The temperature was raised from room temperature to the desired maximum temperature at a rate of 10 °C min^{-1} then held for 30 min (at 800 °C) or 12 h (at 525 °C). Fig. 5 shows the weight change observed during these two temperature ramps (the plots are identical and overlap until 525 °C); below 400 °C little change is observed, however, between 400 °C and 467 °C a weight gain of ~20.5% occurs. Above 480 °C the weight reduces until, in both cases, ~85.5% of the original weight remains. The plots indicate that the conversion of TiC to TiO_2 begins at ~400 °C and continues until ~600 °C; the expected maximum increase is around 33 wt% (M_r TiC = 59.9, M_r TiO_2 = 79.9). Conversely, the combustion of the remaining graphitic component (resulting in weight loss) begins at ~500 °C and continues until the carbon is completely removed. Therefore, assuming complete oxidation, it is possible to estimate that the initial conversion product is ~64 wt% TiC, the remainder being MWCNTs. TGA was used (not shown) to determine the optimal temperature for conversion to anatase of 525 °C; lower temperatures lead to incomplete removal of the remaining carbon, higher temperatures introduce an increasing fraction of rutile.

Highly crystalline, high aspect ratio, oriented arrays of pure TiO_2 nanowires have thus been successfully synthesised, using a simple and readily scalable process. The current aspect ratios are on the order of 1 : 5000. However, CNTs are widely available in a large variety of diameters and lengths (from 1 nm diameter single-walled CNTs to 100 nm MWCNTs). As evidence to confirm the potential versatility of the reaction, we successfully performed conversions of additional CNT samples, including 100 nm diameter nitrogen-doped CNTs[16] and 40 nm diameter CNTs grown using acetylene as the carbon source,[17] to TiC nanorods (see ESI† for TEM images). It can thus be inferred that the reaction is likely provide a generic approach to the production of TiO_2 nanorods with a considerable degree of versatility, leveraging the existing expertise of controlling CNT growth. Pure rutile and almost pure anatase nanorods are produced, although as with other existing approaches to aligned titania nanorods, the products are currently polycrystalline. The mixed crystallinity of the predominantly anatase nanorods may actually be advantageous in certain applications. For some devices, however, there may be a preference for single crystal nanorods and the current approach may provide scope for achieving this goal, since the conversion of CNTs to SiC has previously been shown[4a] to generate single crystal nanorods when performed at 1375 °C. Raising the temperature will provide the additional benefit of favouring full conversion. If the same result can be obtained for TiC, a high yield, coherent conversion to single crystal titania nanorods may be possible.

The authors wish to thank R. Sweeney and J. Cho for XRD analysis. BC acknowledges the EPSRC for funding.

Notes and references

1 (*a*) L. J. E. Hofer, E. Sterling and J. T. McCartney, *J. Phys. Chem.*, 1955, **59**, 1153; (*b*) A. Oberlin, M. Endo and T. J. Toyama, *J. Cryst. Growth*, 1976, **32**, 335.
2 S. Iijima, *Nature*, 1991, **354**, 56.
3 (*a*) P. M. Ajayan and S. Iijima, *Nature*, 1993, **361**, 333; (*b*) P. M. Ajayan, O. Stephan, Ph. Redlich and C. Colliex, *Nature*, 1995, **375**, 564; (*c*) S. C. Tsang, Y. K. Chem, P. J. F. Harris and M. L. H. Green, *Nature*, 1994, **372**, 159; (*d*) C. Guerret-Piecourt, Y. Le Bouar, A. Loiseau and H. Pascard, *Nature*, 1994, **372**, 761.
4 (*a*) C. M. Lieber, S. Fan, H. Dai, E. W. Wong and Y. Z. Lu, *Nature*, 1995, **375**, 769; (*b*) C. M. Lieber, E. W. Wong, B. W. Maynor and L. D. Burns, *Chem. Mater.*, 1996, **8**, 2041.
5 C. E. Snyder, H. W. Mandeville and H. G. Tennent, *Int. Pat.*, WO **89/07163**, 1989.
6 (*a*) W. Z. Li, S. S. Xie, L. X. Qian, B. H. Chang, B. S. Zou, W. Y. Zhou, R. A. Zhao and G. Wang, *Science*, 1996, **274**, 1701; (*b*) M. Terrones, N. Grobert, J. Olivares, J. P. Zhang, H. Terrones, K. Kordatos, W. K. Hsu, J. P. Hare, P. D. Townsend, K. Prassides, A. K. Cheetham, H. W. Kroto and D. R. M. Walton, *Nature*, 1997, **388**, 52; (*c*) Z. F. Ren, Z. P. Huang, J. W. Xu, J. H. Wang, P. Bush, M. P. Siegal and P. N. Provencio, *Science*, 1998, **282**, 1105; (*d*) R. Andrews, D. Jacques, A. M. Rao, F. Derbyshire, D. Qian, X. Fan, E. Dickey and J. Chen, *Chem. Phys. Lett.*, 1999, **303**, 467; (*e*) D. Singh, M. S. P. Shaffer and A. Windle, *Carbon*, 2003, **41**, 359; (*f*) X. Li, A. Cao, Y. J. Jung, R. Vajtai and P. M. Ajayan, *Nano Lett.*, 2005, **5**, 1997.
7 (*a*) P. Hoyer, *Langmuir*, 1996, **12**, 1411; (*b*) S. M. Liu, L. M. Gan, L. H. Liu, W. D. Zhang and H. C. Zeng, *Chem. Mater.*, 2002, **14**, 1391; (*c*) W.-S. Chae, S.-W. Lee and Y.-R Kim, *Chem. Mater.*, 2005, **17**, 3072.
8 (*a*) J. Sun, L. Gao and Q. Zhang, *J. Mater. Sci. Lett.*, 2003, **22**, 339; (*b*) S.-H. Lee, S. Pumprueg, B. Moudgil and W. Sigmund, *Colloids Surf.*, 2005, **B40**, 93; (*c*) D. Eder, I. A. Kinloch and A. H. Windle, *Chem. Commun.*, 2006, **1448.**
9 J. R. Tian, J. A. Voigt, J. Liu, B. McKenzie and H. Xu, *J. Am. Chem. Soc.*, 2003, **125**, 12384.
10 C. Xiong and K. J. Balkus, Jr., *Chem. Mater.*, 2005, **17**, 5136.
11 (*a*) X. Peng and A. Chen, *J. Mater. Chem.*, 2004, **14**, 2542; (*b*) C. Ruan, M. Paulose, O. K. Varghese, G. K. Mor and C. A. Grimes, *J. Phys. Chem. B*, 2005, **109**, 15754; (*c*) J. M. Macak, H. Tsuchiya, L. Taveira, S. Aldabergerova and P. Schmuki, *Angew. Chem., Int. Ed.*, 2005, **44**, 7463; (*d*) C. A. Grimes, *J. Mater. Chem.*, 2007, **17**, 1451.
12 (*a*) S. K. Pradhan, P. J. Reucroft, F. Yang and A. Dozier, *J. Cryst. Growth*, 2003, **256**, 83; (*b*) J.-J. Wu and C.-C. Yu, *J. Phys. Chem. B*, 2004, **108**, 3378.
13 (*a*) M. Graetzel, *Curr. Appl. Phys.*, 2006, **6S1**, e2–e7; (*b*) M. R. Hoffmann, S. T. Marrin, W. Choi and D. W. Bahnemann, *Chem. Rev.*, 1995, **95**, 69.
14 R. Asahi, T. Morikawa, T. Ohwaki, K. Aoki and Y. Yaga, *Science*, 2001, **293**, 269.
15 G. K. Mor, K. Shankar, O. K. Varghese and C. A. Grimes, *J. Mater. Res.*, 2004, **19**, 2989.
16 K. Koziol, M. Shaffer and A. Windle, *Adv. Mater.*, 2005, **17**, 760.
17 H. Cui, G. Eres, J. Y. Howe, A. Puretkzy, M. Varela, D. B. Geohegan and D. H. Lowndes, *Chem. Phys. Rev.*, 2003, **374**, 222.

 This journal is © The Royal Society of Chemistry 2007